

Month 2016 Synthesis of Novel Triazole-incorporated Isatin Derivatives as Antifungal, Antitubercular, and Antioxidant Agents and Molecular Docking Study

Mubarak H. Shaikh,^a Dnyaneshwar D. Subhedar,^a Firoz A. Kalam Khan,^b Jaiprakash N. Sangshetti,^b Laxman Nawale,^c Manisha Arkile,^c Dhiman Sarkar,^c and Bapurao B. Shingate^{a*}

^aDepartment of Chemistry, Dr. Babasaheb Ambedkar Marathwada University, Aurangabad 431 004, India

^bDepartment of Pharmaceutical Chemistry, Y. B. Chavan College of Pharmacy, Dr. Rafiq Zakaria Campus, Aurangabad 431 001, India

^cCombi-Chem Resource Centre, CSIR-National Chemical Laboratory, Pune 411 008, India

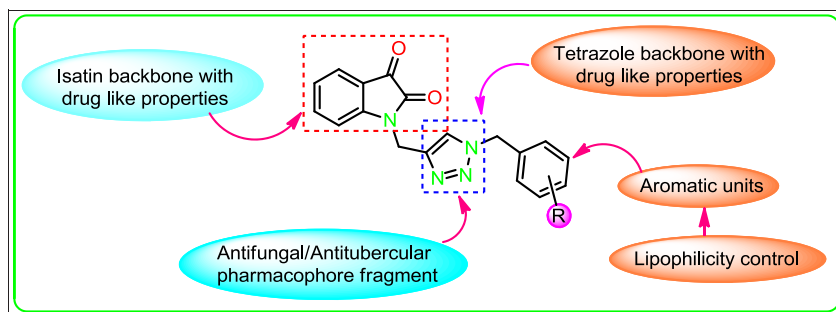
*E-mail: bapushingate@gmail.com

Additional Supporting Information may be found in the online version of this article.

Received September 16, 2015

DOI 10.1002/jhet.2598

Published online 00 Month 2016 in Wiley Online Library (wileyonlinelibrary.com).



A library of 1,2,3-triazoles efficiently prepared via click chemistry and evaluated for their antifungal, antitubercular, antioxidant, cytotoxicity, molecular docking and ADME prediction.

J. Heterocyclic Chem., **00**, 00 (2016).

INTRODUCTION

Recently, the frequency of systemic fungal infection is escalating significantly because of an increase in number of patients undergoing organ transplants, patients with AIDS, and anticancer chemotherapy. Commonly used azole antifungal agents such as voriconazole, fluconazole, itraconazole, and miconazole displayed broad spectrum antifungal activity [1]. Azoles are the drug of choice for antifungal chemotherapy [2] and have broad spectrum activities against most yeasts and filamentous fungi. These antifungal drugs inhibiting CYP51 in the process of biosynthesis of ergosterol through a mechanism in which the heterocyclic nitrogen atom (*N*-4 of triazole) binds to the heme iron atom [3]. However, increasing use of these antifungal drugs has led to increase in resistance to these drugs [4–6]. The 1,4-disubstituted-1,2,3-triazoles with various functionalities/pharmacophoric groups are readily accessible via the copper-catalyzed azide-alkyne cycloaddition as pioneered by Meldal and Sharpless groups [7]. Currently, a few 1,2,3-triazole-based compounds are already in the market or in the final stages of clinical trials [8]. Over the past few years, triazole nucleus present in organic compounds exhibiting antitubercular [9], antibacterial, antiallergic, anti-human immunodeficiency virus (HIV) [10], antifungal [11], and α -glycosidase inhibitor [12] activity. Mostly, 1,2,3-triazole derivatives with regard to

the antitubercular activity have been found to show promising activity profile [13]. The favorable properties of 1,2,3-triazole ring-like hydrogen bonding capability, moderate dipole character, rigidity, and stability under *in vivo* conditions are evidently responsible for their enhanced biological activities [14].

The isatin (1*H*-indole-2,3-dione) moiety is a privileged scaffold, which is responsible for a broad spectrum of biological properties [15] with wide possibility for chemical modification. In this decade, a library of 1,2,3-triazole derivatives conjugated with isatin core structure were synthesized and proved to possess diverse biological activity. Kumar and coworkers synthesized [16] 4-(1,2,3-triazol-1-yl)isatin derivative exhibiting cytotoxic activity against human cancer cell lines. Various isatin–triazole-conjugated systems display antimalarial activity [17], antitrichomoniasis [18], and inhibition potency for caspase-3 [19] were also reported.

Tuberculosis (TB), caused by the pathogen *Mycobacterium tuberculosis* (MTB), is one of the infectious cause of mortality worldwide. The pathogenic synergy between TB and HIV is alarming. Moreover, TB is frequently occurs in HIV/AIDS patients. According to WHO report (2013), 1.5 million deaths were reported because of TB, out of which 0.36 million people were infected with both HIV and TB [20]. Oxidative stress is one of the major causes of tissue inflammation in TB. Because of the poor dietary intake of micronutrients

during illness, the free radicals burst from activated macrophages and anti-TB drugs. Pulmonary inflammation [21] took place if these free radicals were not neutralized by the antioxidants.

In search of this aim, our research efforts have been directed toward the invention of new chemical entities that are effective as antitubercular agents. In continuation of our earlier work [22] on synthesis and biological properties of heterocyclic moieties, herein, we would like to report an elegant synthesis of 1,2,3-triazole-based isatin derivatives via click chemistry and their antimycobacterial activity against MTB H37Ra and antifungal and antioxidant activities with molecular docking study.

RESULTS AND DISCUSSION

Chemistry. We have described the syntheses of new 4-(1,2,3-triazol-1-yl)isatin **9a-g** and **10a-b** derivatives formed by the 1,3-dipolar cycloaddition between aryl azides and isatin-based alkyne via click chemistry approach. The syntheses of starting material benzyl azides **4a-g** were prepared from corresponding benzaldehydes via NaBH₄ reduction and bromination and nucleophilic substitution reaction of sodium azide [23] and azides **6a-b** from corresponding anilines via diazotization followed by azide substitution reaction [24] (Scheme 1).

We have synthesized *N*-propargylindoline-2,3-dione **8** by the treatment of isatin **7** with propargyl bromide in presence of sodium hydride as a base in *N,N*-dimethylformamide (DMF) at room temperature in 85% yield [19] (Scheme 2). Finally, azides **4a-g**, **6a-b**, and *N*-propargylindoline-2,3-dione **8**, on 1,3-dipolar cycloaddition reaction in *t*-BuOH–H₂O (3:1) mixture and catalytic amount of copper diacetate

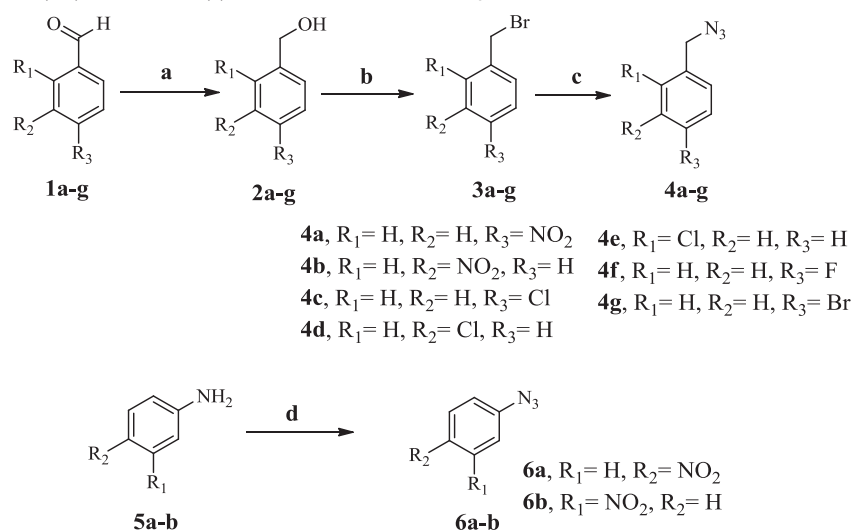
Cu(OAc)₂ at room temperature for 16 to 22 h, afforded the corresponding regioselective 1,4-disubstituted-1,2,3-triazole-incorporated isatin derivatives **9a-g** and **10a-b** in quantitative isolated yield (86–95%) (Scheme 2).

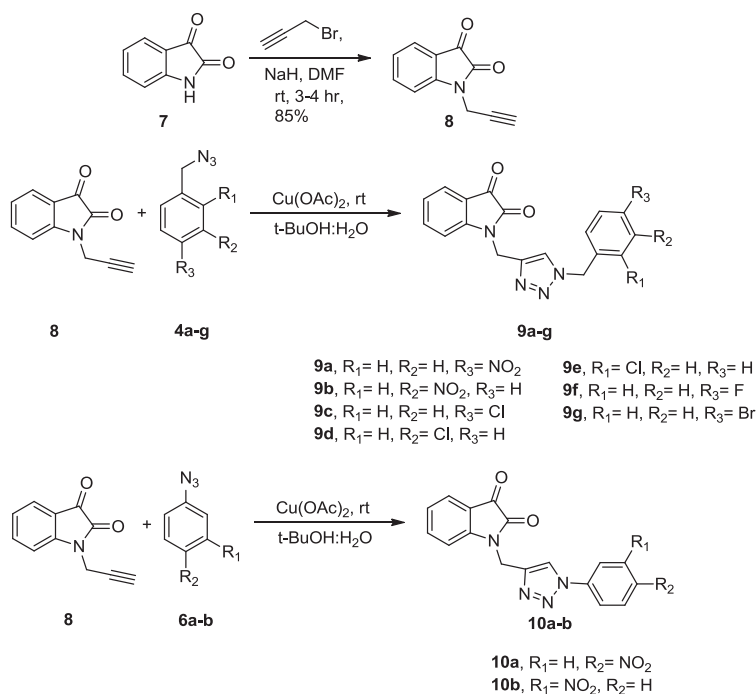
BIOLOGY

Antifungal activity. The synthesized compounds **8**, **9a-g**, and **10a-b** were screened for their *in vitro* antifungal activity. Minimum inhibitory concentration (MIC) values were determined using standard agar method [25]. Dimethyl sulfoxide (DMSO) was used as a solvent or negative control. In order to clarify any effect of DMSO on the biological screening, separate studies were carried out with solutions alone of DMSO and showed no activity against any fungal strains.

In case of antifungal activity, all the synthesized 1,2,3-triazole-based isatin derivatives **9a-g** and **10a-b** show good to moderate activity against all the tested five human pathogenic fungal strains (Table 1). Compound **9a** with *nitro*- group at *para* position of phenyl ring shows equivalent activity against the fungicidal strain *Candida albicans* as compared with standard drug miconazole. The activity of compounds **9d** and **9e** with *chloro*- group at *meta* and *ortho* positions, respectively, of phenyl ring shows potent activity as compared with miconazole against *Fusarium oxysporum*. For *Aspergillus flavus*, compounds **9a** with *nitro*- group at *para*, **9d** with *chloro*- group at *meta*, and **9f** with *fluoro*- group at *para* position of phenyl ring show comparable activity as compared with miconazole. Compound **9a** with an MIC value of 25 µg/mL possesses equivalent activity compared with standard drug miconazole. Again, compounds **9b** and **9i** having *nitro*- substituent

Scheme 1. Synthetic route for target compounds **4a-g** and **6a-b**. Reagents and conditions: (a) NaBH₄, methanol, 0°C to rt, 2 h; (b) PBr₃, DCM, 0°C, 0.5 h; (c) NaN₃, acetone:H₂O (3:1), rt, 24 h; and (d) NaNO₂, HCl, 0°C then NaN₃.



Scheme 2. Synthetic route for triazole-incorporated isatin derivatives **9a-g** and **10a-b**.

at *meta* position of phenyl ring show promising activity as compared with the standard drug miconazole. However, none of the synthesized compounds show promising antifungal activity compared with the standard antifungal drug fluconazole. The starting material *N*-propargylindoline-2,3-dione **8** does not show any antifungal activity against all the tested fungal strains. However, after introduction of 1,2,3-triazole ring on isatin, it gave remarkable antifungal activity.

Antitubercular activity. The synthesized 1,4-disubstituted-1,2,3-triazoles **9a-g** and **10a-b** were screened for *in vitro* antitubercular activity against MTB H37Ra (ATCC 25177) in liquid medium using XRMA protocol [26]. The primary screening data for compounds **9a-g** and **10a-b** are shown in the Supporting Information (Tables S1 and S2). In particular, the compounds **9e**, **9f**, **9g**, **10a**, and **10b** were found to be active against MTB H37Ra strain. The IC₉₀

Table 1

In vitro antitubercular activity against MTB H37Ra, antifungal activity and DPPH radical scavenging activity of compounds **8** and **9a-g** and **10a-b**.

Entry	Anti TB IC ₉₀ (μg/mL) MTB H37Ra	DPPH IC ₅₀ (μg/mL)	Antifungal activity MIC values (μg/mL)				
			CA	FO	AF	AN	CN
8	54.66 ± 0.80	37.40	*	*	*	*	*
9a	>30	44.12	25	50	25	25	100
9b	>30	66.15	150	100	50	50	25
9c	>30	64.29	125	125	125	*	*
9d	87.02 ± 0.98	55.63	*	25	25	37.5	150
9e	28.53 ± 0.10	16.35	50	25	150	*	*
9f	29.05 ± 0.09	14.14	50	50	25	*	*
9g	8.09 ± 0.63	66.26	37.5	150	87.5	50	150
10a	26.65 ± 0.83	74.29	50	150	150	100	*
10b	7.56 ± 0.24	57.11	150	150	50	100	25
Rifampicin	0.043 ± 0.0015	NT	NT	NT	NT	NT	NT
Isoniazid	0.075 ± 0.0025	NT	NT	NT	NT	NT	NT
BHT	NT	16.47	NT	NT	NT	NT	NT
Miconazole	NT	NT	25	25	12.5	25	25
Fluconazole	NT	NT	12.5	6.25	6.25	12.5	6.25

*Activity was not observed up to 200 μg/mL.

CA, *Candida albicans*; FO, *Fusarium oxysporum*; AF, *Aspergillus flavus*; AN, *Aspergillus niger*; CN, *Cryptococcus neoformans*; BHT, butylated hydroxy toluene; NT, not tested.

values of compounds **9a–g** and **10a–b** were observed in the range of 7.56–87.02 $\mu\text{g/mL}$, which implies their potential as promising antitubercular agents (Table 1).

Most of the synthesized compounds exhibit good to excellent antitubercular activity as compared with the standard drugs. However, compound **10b** ($\text{IC}_{90}=7.56 \mu\text{g/mL}$) shows the highest activity as compared with the other synthesized compounds. Compound **9g** ($\text{IC}_{90}=8.09 \mu\text{g/mL}$) with *bromo-* group at *para* position of phenyl ring shows better activity. Compounds **9e** ($\text{IC}_{90}=28.53 \mu\text{g/mL}$) and **10a** ($\text{IC}_{90}=26.65 \mu\text{g/mL}$) with *chloro-* group at *ortho* and *nitro-* group at *para* position, respectively, of phenyl rings display better activity. The bactericidal effect of the **9g** and **10b** on dormant bacilli revealed that **9g** and **10b** possess higher anti-dormancy activity than the compounds **9e**, **9f**, and **10a**. The substitution at *para* position on phenyl ring is important for the antitubercular activity. When at *para* position of phenyl ring, *nitro-* (compound **9a**) and *chloro-* (compound **9c**) groups are present at that time compound exhibited MIC values more than 30 $\mu\text{g/mL}$. Similarly, when *fluoro-* (compound **9f**) group is present at *para* position, it exhibited antitubercular activity with MIC $29.05 \pm 0.09 \mu\text{g/mL}$. Moreover, when *para* position is substituted by *bromo-* group (compound **9g**), then the compound exhibited excellent antitubercular activity with an MIC value of $8.09 \pm 0.63 \mu\text{g/mL}$. Other compounds also display significant antitubercular activity (both IC_{90} and IC_{50}) against dormant phase (Supporting Information Table S2). Therefore, the overall antitubercular activity exhibited in this study by the given set of compounds varied from weak to significant.

Antioxidant activity. 1,1-Diphenyl-1-picrylhydrazyl (DPPH) radical scavenging activity [27] is the most commonly used method for screening antioxidant activities of the various natural as well as synthetic antioxidants. A lower IC_{50} value indicates a greater antioxidant activity. The IC_{50} values, which are the concentration required to scavenge 50% of the radicals, were calculated to evaluate the potential antioxidant activities. The IC_{50} of butylated hydroxytoluene (BHT) was considered for comparison. The results were summarized in Table 1. In DPPH assay, compounds **9e** with *chloro-* group at *ortho* and **9f** with *fluoro-* group at *para* position of phenyl ring exhibit excellent radical scavenging activity than the standard antioxidant BHT, with IC_{50} values of 16.35 and 14.14 $\mu\text{g/mL}$, respectively. The position of *chloro-* group on phenyl ring is important for the antioxidant activity. In compounds **9c** ($\text{IC}_{50}=64.29 \mu\text{g/mL}$) and **9d** ($\text{IC}_{50}=55.63 \mu\text{g/mL}$), the *chloro-* group at *para* and *meta* position of phenyl ring, respectively, showed less antioxidant activity compared with compound **9e** ($\text{IC}_{50}=16.35 \mu\text{g/mL}$) where *chloro-* group is present at *ortho* position of phenyl ring. The substitution of R_3 with bromine (compound **9g**, $\text{IC}_{50}=66.26 \mu\text{g/mL}$) led to

decrease in activity when compared with *fluoro-* substitution at R_3 in compound **9f** ($\text{IC}_{50}=14.14 \mu\text{g/mL}$). Among the synthesized triazole-incorporated isatin derivatives, **10a** exhibits the lowest activity with an IC_{50} value of 74.29 $\mu\text{g/mL}$. From these observations, we can conclude that the phenyl ring having *chloro-* group at *ortho* and *fluoro-* group at *para* position shows promising DPPH radical scavenging activity.

Cytotoxic activity. The compounds **9e**, **9f**, **9g**, **10a**, and **10b**, which displayed antitubercular activity, were further assayed for their cytotoxicity in three different human cancer cell lines A549 (human lung adenocarcinoma epithelial cell line), PANC-1 (human pancreas carcinoma cell line), and HeLa (human cervix epithelial carcinoma cell line), using MTT assay [28] with 48-h exposure time of the tested compounds, and paclitaxel was used as positive control.

The cytotoxic effect of these compounds was checked on cancer cell lines using the concentration range between 100 and 0.78 $\mu\text{g/mL}$ to determine the GI_{50} and GI_{90} (Table 2). A perusal of this table revealed that compounds (**9e**, **9f**, **9g**, **10a**, and **10b**) are least cytotoxic up to 100 $\mu\text{g/mL}$ on A549 and PANC-1 cell lines used.

COMPUTATIONAL STUDY

Molecular docking. The synthesized compounds **9a–g** and **10a–b** and standard drug (fluconazole) were docked into the active site of cytochrome P450 lanosterol 14 α -demethylase of *C. albicans* using VLifeMDS 4.3 software (VLife Technologies, a division of NovaLead Pharma Pvt. Ltd., Pune, Maharashtra, India) package to understand the binding interactions. The docking interactions of active compounds **9a** and **9g** and least active compound **9b** and fluconazole (standard drug) are shown in Figure 1. The most active compounds **9a** ($\text{MIC}=25 \mu\text{g/mL}$) and **9g** ($\text{MIC}=37.5 \mu\text{g/mL}$) have shown good binding energies of -69.02 and -63.71 kcal/mol , respectively. The docking result indicates that the synthesized compounds were detained in the active pocket by forming various hydrophobic bonds and van der Waals interactions with the enzyme. In case of compound **9a**, the isatin–triazole core was held in active pocket by forming various hydrophobic and van der Waals interactions with amino acid residues, viz. ALA343, THR347, LEU412, PHE499, GLY500, HIS504, ARG505, CYS506, ILE507, and GLY508. The *nitro-* group at *para* position in compound **9a** was also well fitted into active site by forming the van der Waals interactions with amino acids PHE141, SER414, MET415, and PRO442. The compound **9g** was held in active pocket of enzyme by forming various hydrophobic and van der Waals interactions with amino acid residues like PHE141, TYR154, ALA343, LEU412, MET415, PHE416, VAL440,

Table 2

Cytotoxicity of selected compounds in three human cancer cell lines^a.

Compound	Cytotoxic profile against human cancer cell lines with SD values					
	A549		PANC-1		HeLa	
	GI ₅₀	GI ₉₀	GI ₅₀	GI ₉₀	GI ₅₀	GI ₉₀
9e	>100 ± 0.71	>100 ± 0.01	>100 ± 0.01	>100 ± 0.90	41.62 ± 0.55	>100 ± 0.75
9f	>100 ± 0.39	>100 ± 0.57	>100 ± 0.17	>100 ± 0.90	20.26 ± 0.94	72.80 ± 0.80
9g	>100 ± 0.62	>100 ± 0.30	>100 ± 0.99	>100 ± 0.46	03.41 ± 0.90	28.05 ± 0.26
10a	>100 ± 0.63	>100 ± 0.87	>100 ± 0.41	>100 ± 0.21	25.41 ± 0.91	>100 ± 0.81
10b	>100 ± 0.52	>100 ± 0.64	>100 ± 0.03	>100 ± 0.43	04.56 ± 0.51	36.54 ± 0.17
^b Paclitaxel	0.14 ± 0.53	5.81 ± 0.02	0.13 ± 0.96	5.72 ± 0.19	0.01 ± 0.71	0.07 ± 0.60

^aGI₅₀/GI₉₀ in microgram per milliliter, after 48 h. Human cancer cell lines: A549 from lung adenocarcinoma, PANC-1 from pancreas carcinoma, and HeLa from cervix carcinoma. Results show that cell viability >80% at the highest concentration of 100 µg/mL.

^bStandard anticancer drug and positive control. The GI₅₀ values were indicated as mean calculated from three independent experiments.

SER441, PRO442, PHE499, GLY500, and HIS504. The *bromo-* group at *para* position in compound **9g** formed two van der Waals interactions with amino acid ALA343. Thus, bulky substituents like *nitro-* and *bromo-* were detained deep into active site of enzyme and responsible for good antifungal activity. In case of least active compound **9b**, the compound had shown poor interactions with binding energy -43.42 kcal/mol. The compound **9b** was held in active pocket by forming various hydrophobic and van der Waals interactions with amino acid residues: TYR154, ALA343, THR347, LEU412, MET415, PHE416, PRO498, PHE499, GLY500, HIS504, ARG505, CYS506, GLY508, and ALA512. On the basis of activity data and docking results, it has been found that the compounds **9a** and **9g** have potential to inhibit 14 α -demethylase of *C. albicans*.

In silico absorption, distribution, metabolism, and excretion prediction. The sensation of a drug is determined by an acceptable absorption (ABS), distribution, metabolism, and excretion (ADME) profile and its efficacy. It is observed that all the synthesized compounds exhibited a good percentage absorption (% ABS) ranging from 69.11 to 95.52% (Table 3).

The pharmacokinetic data obtained for all the synthesized compounds **8**, **9a-g**, and **10a-b** were within the range of accepted values. From all these parameters, it can be observed that all titled compounds exhibited a good % ABS (69.11–95.52%). Furthermore, none of the synthesized compounds violated Lipinski's rule of five, thus showing possible utility of series for developing the compound with good drug-like properties. A molecule likely to be developed as an orally active drug candidate should show no more than one violation of the following four criteria: *miLog P* (octanol–water partition coefficient) ≤ 5 , molecular weight ≤ 500 , number of hydrogen bond acceptors ≤ 10 , and number of hydrogen bond donors ≤ 5 [29]. All the synthesized compounds followed the criteria for orally active drug, and therefore, these compounds can be further developed as oral drug candidates.

EXPERIMENTAL

All the reagents and solvents were purchased from commercial suppliers Spectrochem (Spectrochem Pvt. Ltd., Mumbai, India), Rankem (Avantor Performance Material India Limited, Thane, Maharashtra, India), Alfa Aesar (Thermo Fisher Scientific, Hyderabad, India), and Sigma Aldrich (Bengaluru, Kamataka, India) and are used without further purification. Reaction time and purity of the products were observed by thin-layer chromatography (TLC) aluminum sheets, silica gel 60-F₂₅₄ precoated, Merck, Germany, and spots were located by using UV light or iodine vapors as the visualizing agent. All the melting points were found out in an open capillary method and are uncorrected. ¹H NMR spectra were recorded on Jeol 400-MHz spectrometer and ¹³C NMR on 100-MHz spectrometer (JEOL USA, Inc., Peabody, MA) using residual solvent as internal standard (CDCl₃). The chemical shifts (δ) were reported and are given in parts per million (ppm). The splitting pattern abbreviations are designed as singlet (s), doublet (d), double doublet (dd), triplet (t), quartet (q), and multiplet (m). Mass spectra were recorded on micrOTOF-Q II spectrometer (Bruker, Billerica, MA) in the electrospray ionization modes.

Synthesis of *N*-propargylindoline-2,3-dione (8**).** In a 50-mL round bottom flask, sodium hydride (1.5 mmol) in dry DMF (10 mL) and isatin **7** (1 mmol) were added and allowed to stir at room temperature, resulting in the formation of purple colored anion. The solution was stirred till the evolution of hydrogen ceases. Then to this reaction mixture drop wise, a solution of propargyl bromide (1.1 mmol) in DMF was added and allowed to constant stirring for about 2 h. The progress of the reaction was monitored by TLC using ethyl acetate:hexane as a solvent system. The reaction mixture was quenched with crushed ice and extracted with ethyl acetate (3 × 30 mL). The combined organic layers were washed with brine solution and dried over anhydrous sodium sulphate. The solvent was evaporated under reduced pressure to afford the

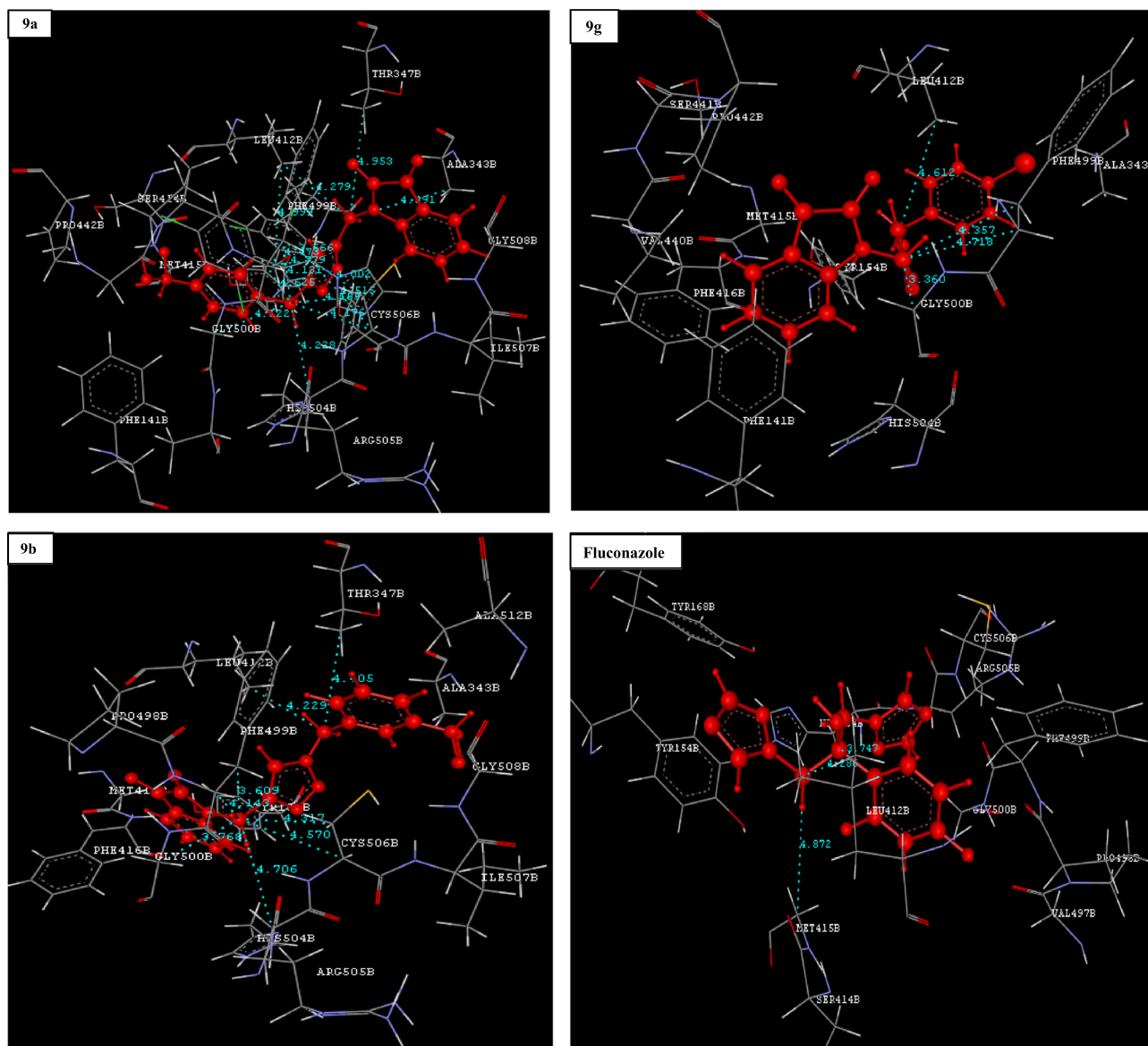


Figure 1. Docking images of the most active compounds **9a** and **9g**, the most inactive compound **9b**, and standard antifungal drug fluconazole. Hydrogen bonds are shown in green color. Ligands are shown in red color. Hydrophobic bonds are shown in sky blue color. [Color figure can be viewed in the online issue, which is available at [wileyonlinelibrary.com](http://www.wileyonlinelibrary.com).]

corresponding crude compound, which is crystallized in aq. ethanol to furnish the desired *N*-propargylated isatin (**8**) in 85% yield, mp 156–158°C.

General procedure for the synthesis of 4-(1,2,3-triazol-1-yl)isatin derivatives (9a–g) and (10a–b). To the stirred solution of *N*-propargylindoline-2,3-dione (**8**) (0.5 mmol), benzyl azide **4a–g** and **6a–b** (0.5 mmol) and catalytic amount of copper diacetate ($\text{Cu}(\text{OAc})_2$) (20 mole %) in *t*-BuOH- H_2O (3:1, 12 mL) were added at room temperature and allowed stirring for 16–22 h. The progress of the reaction was observed by TLC using ethyl acetate:hexane as a solvent system. After completion of reaction indicated by TLC, the reaction mixture was quenched with crushed ice and

extracted with ethyl acetate (2 × 15 mL). The organic extracts were washed with brine solution (2 × 15 mL) and dried over anhydrous sodium sulphate. The solvent was evaporated under reduced pressure to afford the corresponding crude compounds, which was recrystallized using ethanol.

1-((1-(4-Nitrobenzyl)-1H-1,2,3-triazol-4-yl)methyl)indoline-2,3-dione (9a). The compound was obtained from **4a** and **8** as orange solid, yield 95%, mp 216°C; ^1H NMR (400 MHz, CDCl_3): δ_{H} ppm 5.01 (s, 2H, N- CH_2), 5.60 (s, 2H, N- CH_2), 7.11–7.14 (t, 1H, ArH), 7.29–7.31 (d, 1H, $J=8$ Hz, ArH), 7.40–7.42 (d, 2H, $J=8$ Hz, ArH), 7.57–7.60 (m, 2H, ArH), 7.65 (s, 1H, triazole ring), 8.21–8.23 (d, 2H, $J=8$ Hz, ArH). HRMS calculated $[\text{M}+\text{Na}]^+$ for $\text{C}_{18}\text{H}_{13}\text{N}_5\text{O}_4\text{Na}$: 386.0869,

Table 3

Pharmacokinetic parameters important for good oral bioavailability.

Entry Rule	% ABS	TPSA (Å ²)	n-ROTB	MV	MW <500	miLog P ≤5	n-ON acceptors <10	n-OHND donors <5	Lipinski violation ≤1
8	95.52	39.07	1	163.01	185.18	1.05	3	0	0
9a	69.11	115.61	5	300.76	363.33	2.20	9	0	0
9b	69.11	115.61	5	300.76	363.33	2.17	9	0	0
9c	84.92	69.79	4	290.96	352.78	2.92	6	0	0
9d	84.92	69.79	4	290.96	352.78	2.89	6	0	0
9e	84.92	69.79	4	290.96	352.78	2.87	6	0	0
9f	84.92	69.79	4	282.35	336.32	3.76	6	0	0
9g	68.92	69.79	4	295.31	397.23	3.05	6	0	0
10a	69.11	115.61	4	283.96	349.30	1.88	9	0	0
10b	69.11	115.61	4	283.96	349.30	2.06	9	0	0

% ABS, percentage absorption; TPSA, topological polar surface area; n-ROTB, number of rotatable bonds; MV, molecular volume; MW, molecular weight; miLog P, logarithm of partition coefficient of compound between n-octanol and water; n-ON acceptors, number of hydrogen bond acceptors; n-OHND donors, number of hydrogen bonds donors.

found: 386.0869, and $[M+K]^+$ for $C_{18}H_{13}N_5O_4K$: 402.0608, found: 402.0609.

1-((1-(3-Nitrobenzyl)-1H-1,2,3-triazol-4-yl)methyl)indoline-2,3-dione (9b). The compound was obtained from **4b** and **8** as orange solid, yield 93%, mp 206°C; ¹H NMR (400 MHz, CDCl₃): δ_H ppm 5.02 (s, 2H, N-CH₂), 5.60 (s, 2H, N-CH₂), 7.10–7.14 (t, 1H, ArH), 7.29–7.31 (d, 2H, J=8 Hz, ArH), 7.55–7.63 (m, 5H, ArH), 8.12 (s, 1H, triazole ring), 8.21–8.23 (m, 1H, ArH); ¹³C NMR (100 MHz, CDCl₃): δ_C ppm 53.7, 111.6, 116.2, 116.4, 117.6, 122.8, 124.1, 125.4, 130.3, 138.7, 142.3, 150.3, 158, 161.8, 164.3, 183.1. HRMS calculated $[M+Na]^+$ for $C_{18}H_{13}N_5O_4Na$: 386.0869, found: 386.0869, and $[M+K]^+$ for $C_{18}H_{13}N_5O_4K$: 402.0608, found: 402.0609.

1-((1-(4-Chlorobenzyl)-1H-1,2,3-triazol-4-yl)methyl)indoline-2,3-dione (9c). The compound was obtained from **4c** and **8** as orange solid, yield 94%, mp 206–208°C; ¹H NMR (400 MHz, CDCl₃): δ_H ppm 4.99 (s, 2H, N-CH₂), 5.45 (s, 2H, N-CH₂), 7.09–7.13 (t, 1H, ArH), 7.18–7.21 (m, 2H, ArH), 7.29–7.35 (m, 3H, ArH), 7.54 (s, 1H, triazole ring), 7.56–7.60 (m, 2H, ArH). MALDI-TOF for $C_{18}H_{14}ClN_4O_2$ calculated $[M+H]^+$ is 353.0805 and $[M+H]^+$ observed at 353.2561. Calculated $[M+Na]^+$ $C_{18}H_{13}ClN_4O_2Na$ is 375.0625 and observed $[M+Na]^+$ at 375.2400.

1-((1-(3-Chlorobenzyl)-1H-1,2,3-triazol-4-yl)methyl)indoline-2,3-dione (9d). The compound was obtained from **4d** and **8** as orange solid, yield 89%, mp 136–138°C; ¹H NMR (400 MHz, CDCl₃): δ_H ppm 4.99 (s, 2H, N-CH₂), 5.45 (s, 2H, N-CH₂), 7.10–7.13 (t, 1H, ArH), 7.19–7.21 (d, 2H, J=8 Hz, ArH), 7.30–7.35 (m, 3H, ArH), 7.54 (s, 1H, triazole ring), 7.57–7.60 (m, 2H, ArH); ¹³C NMR (100 MHz, CDCl₃): δ_C ppm 53.8, 111.6, 117.6, 123, 124.2, 125.5, 129.6, 132.6, 135.2, 138.8, 142.4, 150.3, 183.1. MALDI-TOF for $C_{18}H_{14}ClN_4O_2$ calculated $[M+H]^+$ is 353.0805 and $[M+H]^+$ observed at 353.2798. Calculated $[M+Na]^+$ $C_{18}H_{13}ClN_4O_2Na$ is 375.0625 and observed $[M+Na]^+$ at 375.2494.

1-((1-(2-Chlorobenzyl)-1H-1,2,3-triazol-4-yl)methyl)indoline-2,3-dione (9e). The compound was obtained from **4e** and **8**

as orange solid, yield 86%, mp 100°C. MALDI-TOF for $C_{18}H_{14}ClN_4O_2$ calculated $[M+H]^+$ is 353.0805 and $[M+H]^+$ observed at 353.2440. Calculated $[M+Na]^+$ $C_{18}H_{13}ClN_4O_2Na$ is 375.0625 and observed $[M+Na]^+$ at 375.2343.

1-((1-(4-Fluorobenzyl)-1H-1,2,3-triazol-4-yl)methyl)indoline-2,3-dione (9f). The compound was obtained from **4f** and **8** as orange solid, yield 94%, mp 180°C; ¹H NMR (400 MHz, CDCl₃): δ_H ppm 4.98 (s, 2H, N-CH₂), 5.45 (s, 2H, N-CH₂), 7.03–7.13 (m, 3H, ArH), 7.24–7.32 (m, 3H, ArH), 7.53–7.60 (m, 3H, ArH). HRMS calculated $[M+H]^+$ for $C_{18}H_{14}N_4O_2F$: 337.1060, found: 337.1057, and $[M+Na]^+$ for $C_{18}H_{13}N_4O_2FNa$: 359.0880, found: 359.0880.

1-((1-(4-Bromobenzyl)-1H-1,2,3-triazol-4-yl)methyl)indoline-2,3-dione (9g). The compound was obtained from **4g** and **8** as orange solid, yield 92%, mp 204°C; ¹H NMR (400 MHz, CDCl₃): δ_H ppm 4.99 (s, 2H, N-CH₂), 5.45 (s, 2H, N-CH₂), 7.03–7.13 (m, 3H, ArH), 7.24–7.32 (m, 3H, ArH), 7.53–7.60 (m, 3H, ArH); ¹³C NMR (100 MHz, CDCl₃): δ_C ppm 53.8, 111.6, 116.3, 117.6, 122.9, 124.2, 125.5, 130.3, 138.8, 142.3, 150.3, 158.1, 161.8, 164.3, 183.2. HRMS calculated $[M+K]^+$ for $C_{18}H_{13}N_4O_2K$: 436.1891, found: 436.0094.

1-((1-(4-Nitrophenyl)-1H-1,2,3-triazol-4-yl)methyl)indoline-2,3-dione (10a). The compound was obtained from **6a** and **8** as orange solid, yield 88%, mp 210°C; ¹H NMR (400 MHz, CDCl₃): δ_H ppm 4.98 (s, 2H, N-CH₂), 7.03–7.13 (m, 3H, ArH), 7.24–7.32 (m, 3H, ArH); 7.53–7.60 (m, 3H, ArH). HRMS calculated $[M+K]^+$ for $C_{17}H_{11}N_5O_4K$: 388.0403, found: 388.0403.

1-((1-(3-Nitrophenyl)-1H-1,2,3-triazol-4-yl)methyl)indoline-2,3-dione (10b). The compound was obtained from **6b** and **8** as orange solid, yield 86%, mp 230°C; ¹H NMR (400 MHz, CDCl₃): δ_H ppm 5.01 (s, 2H, N-CH₂), 7.11–7.14 (t, 1H, ArH), 7.29–7.31 (d, 1H, J=8 Hz, ArH), 7.40–7.42 (d, 2H, J=8 Hz, ArH); 7.57–7.60 (m, 2H, ArH), 7.65 (s, 1H, triazole ring), 8.21–8.23 (d, 2H, J=8 Hz, ArH); ¹³C NMR (100 MHz, CDCl₃): δ_C ppm 53.4, 111.4, 117.6, 123.3,

124.5, 125.5, 128.9, 138.8, 141.1, 142.7, 150.2, 158.1, 183.1.
HRMS calculated $[M+K]^+$ for $C_{17}H_{11}N_5O_4K$: 388.0403,
found: 388.0403.

CONCLUSION

In summary, we have synthesized new triazole-based isatin derivatives via click chemistry and evaluated for biological activity. The synthesized compounds show promising antifungal, antitubercular, antioxidant, and nonantiproliferative activity as compared with the respective standard drugs. Compound **9a** displayed significant antifungal activity as compared with the standard antifungal drug miconazole. Compounds **9g** and **10b** show antitubercular activity with an IC_{90} of value 8.09, and 7.56 $\mu\text{g/mL}$ is capable with maximum potency, which is threefold times more active than **9e**, **9f**, and **10a** against the strain MTB H37Ra. Compound **9f** shows potential antioxidant activity ($IC_{50} = 14.14 \mu\text{g/mL}$) as compared with standard drug BHT. This study shows that compounds **9e**, **9f**, **9g**, **10a**, and **10b** have low cytotoxicity (nil up to 100 $\mu\text{g/mL}$) against human cancer cell lines A549 and PANC-1. However, molecular docking study of these synthesized triazole derivatives has shown a high affinity towards the active site of enzyme cytochrome P450 lanosterol 14 α -demethylase. In addition to this, the analysis of ADME parameters for triazole-based isatin derivatives possesses good drug-like properties that can be developed as oral drug contestant. Thus, suggesting that the compounds from present series **9a** (antifungal activity), **9g** and **10b** (antitubercular), and **9f** (antioxidant activity) can be further optimized and developed as a lead molecule.

EXPERIMENTAL PROTOCOL FOR BIOLOGICAL ACTIVITY

Antifungal activity. The antifungal activity was tested against five human pathogenic fungal strains, such as *C. albicans* (NCIM 3471), *F. oxysporum* (NCIM 1332), *A. flavus* (NCIM 539), *Aspergillus niger* (NCIM 1196), and *Cryptococcus neoformans* (NCIM 576), and results were compared with standard antifungal drug miconazole. Standard agar method was used to determine the MIC values [25].

Antitubercular activity by XRMA protocol. All the synthesized compounds **8**, **9a–g**, and **10a–b** were evaluated for their *in vitro* effects against dormant-phase MTB H37Ra using XRMA protocol [26]. IC_{50} and MIC values were calculated from their dose–response curves, and all the experiments were performed in triplicates.

$$\% \text{ Inhibition} = 100 - (A_1 - \text{Blank}) / (A_2 - \text{Blank}) \times 100$$

where A_1 is the culture absorbance at 470 nm in the presence of the compound after addition of menadione, A_2 is

the culture absorbance at 470 nm (DMSO solvent control) after addition of menadione, and Blank is the culture absorbance at 470 nm of the respective data points before addition of 2,3-bis-(2-methoxy-4-nitro-5-sulfophenyl)-2H-tetrazolium-5-carboxanilide (XTT)/menadione.

1,1-Diphenyl-1-picrylhydrazyl radical scavenging activity. The bleaching of the purple colored methanol solution of DPPH radical scavenging activity [27] was used for the determination of hydrogen atom or electron donation ability of the compounds. The stable radical DPPH used as a reagent in spectrophotometric assay. 1 mL of various concentrations of the test compounds (5, 10, 25, 50 and 100 $\mu\text{g/mL}$) in methanol was added to 4 mL of 0.004% (w/v) methanol solution of DPPH. At room temperature after a 30 min incubation period, the absorbance was measured against blank at 517 nm. The percent inhibition (I %) of free radical production from DPPH was calculated by the following equation.

$$\% \text{ of scavenging} = [(A \text{ control} - A \text{ sample}) / A \text{ blank}] \times 100$$

where “A control” is the absorbance of the control reaction (containing all reagents except the test compound) and “A sample” is the absorbance of the test compound. Tests were carried out in triplicate.

Cytotoxic activity assay. The effect of compounds **8**, **9a–g**, and **10a–b** was examined on cell growth in lung A549 adenocarcinoma, pancreatic PANC-1 adenocarcinoma cell line, and HeLa cell lines. Standard MTT [3-(4,5-dimethylthiazol-2-yl)-2,5-diphenyltetrazolium bromide] assay [28] for measuring cellular proliferation was used for measuring the cytotoxicity on three human cancer cell lines. In a single experiment, each concentration was tested in triplicates. The viability and growth in the presence of test material are calculated by as follows: (% cytotoxicity = (Average of control – Average of compound) / (Average of control – Average of blank) \times 100), where control is a culture medium with cells and DMSO and blank is a culture medium without cells.

IC_{50} and MIC values were calculated by plotting the percentage survival versus the concentrations, using OriginPro software (Adalta, Arezzo, Italy).

Molecular docking study. Molecular docking study was carried out using VLife MDS 4.3 package. In view of this, to prepare protein for docking study, crystal structure of DprE1 (decaprenylphosphoryl- β -D-ribose-2'-epimerase) enzyme of MTB (PDB ID: 4FDO) was obtained from the Protein Data Bank. The standard protocol implemented in VLife MDS 4.3 package was used for docking procedure, and the compounds were docked against three-dimensional structure of DprE1 enzyme. The 3D model structure of cytochrome P450 lanosterol 14 α -demethylase of *C. albicans* was constructed using homology modeling with the help of VLifeMDS 4.3 ProModel. From the Universal Protein Resource

(<http://www.uniprot.org/>) (Accession Code: P10613), amino acid sequence of enzyme was obtained, and from Protein Data Bank using Blast search, homologous sequence was obtained. Based on the result of blast search, we used the crystal structure of human lanosterol 14 α -demethylase (CYP51) with azole as a template for homology modeling (PDB ID: 3LD6) [30]. The alignment of amino acid sequence of CA-CYP51 (P10613) and human CYP51 (3LD6_B) was performed. The parameters like sequence identities and sequence positives are important for the selection of template structure. The sequence identities and sequence positives were found to be 39 and 54%, which satisfy the basic criteria for comparative modeling (Figure S1, Supporting Information). The quality of generated *C. albicans* lanosterol 14 α -demethylase model was assessed by using the well-validated program likes PROCHECK [31], and its structural validation is shown in Figure S2 (Supporting Information). It was found that residue were followed, 82.45% in core region, 11.42% in allowed region, and 4.44% in generously allowed region. The only 1.69% residues were found in disallowed region. The further structural superimposition was performed to know the structural coordinate of target protein, and root-mean-square deviation value was found within a standard range of 0.997607 Å. The validation study of the model suggested that it was perfect for further computation study.

Absorption, distribution, metabolism, and excretion prediction. All the synthesized compounds **8**, **9a–g**, and **10a–b** were evaluated by computational study for prediction of ADME properties. In this computational study, we have calculated topological polar surface area (TPSA), number of rotatable bonds, molecular volume, molecular weight, logarithm of partition coefficient (miLog *P*), number of hydrogen bond acceptors, number of hydrogen bond donors, and Lipinski's rule of five using Molinspiration online property calculation toolkit. Percentage ABS was calculated as follows: % ABS = 109 – (0.345 × TPSA).

Acknowledgments. The authors M.H.S. and D.D.S. are very much grateful to the Council of Scientific and Industrial Research (CSIR), New Delhi, for the award of Senior Research Fellowship. Authors are also thankful to the Head, Department of Chemistry, Dr. Babasaheb Ambedkar Marathwada University, Aurangabad, for providing laboratory facility.

REFERENCES AND NOTES

- [1] Sheehan, D. J.; Hitchcock, C. A.; Sibley, C. M. *Clin Microbiol Rev* 1999, 12, 40.
- [2] Cha, R.; Sobel, J. D. *Expert Rev Anti Infect Ther* 2004, 2, 357.
- [3] Georgopadakou, N. H.; Walsh, T. J. *Antimicrob Agents Chemo Ther* 1996, 40, 279.
- [4] Pfaller, M. A.; Messer, S. A.; Hollis, R. J.; Jones, R. *J Antimicrob Agents Chemo Ther* 2001, 45, 2862.
- [5] Jeu, L.; Piacenti, F. J.; Lyakhovetskiy, A. G.; Fung, H. B. *Clin Ther* 2003, 25, 1321.
- [6] Lepesheva, G. I.; Zaitseva, N. G.; Nes, W. D.; Zhou, W.; Arase, M.; Liu, J.; Hill, G. C.; Waterman, M. R. *J Biol Chem* 2014, 281, 3577.
- [7] (a) Tornøe, C. W.; Christensen, C.; Meldal, M. *J Org Chem* 2002, 67, 3057; (b) Rostovtsev, V. V.; Green, L. G.; Fokin, V. V.; Sharpless, K. B. *Angew Chem Int Ed* 2002, 41, 2596.
- [8] Therrien, C.; Levesque, R. C. *FEMS Microbiol Rev* 2000, 24, 251.
- [9] Boechat, N.; Ferreira, V. F.; Ferreira, S. B.; Ferreira, M. L. G.; da Silva, F. C.; Bastos, M. M.; Costa, M. S.; Lourenco, M. C. S.; Pinto, A. C.; Kretli, A. U.; Aguiar, A. C.; Teixeira, B. M.; da Silva, N. V.; Martins, P. R. C.; Bezerra, F. A. F. M.; Camilo, A. L. S.; da Silva, G. P.; Costa, C. C. P. *J Med Chem* 2011, 54, 5988.
- [10] Agalave, S. G.; Maujan, R. S.; Pore, V. S. *Chem Asian J* 2011, 6, 2696 and references cited therein.
- [11] Lima-Neto, R. G.; Cavalcante, N. N. M.; Srivastava, R. M.; Mendonca, F. J. B.; Wanderley, A. G.; Neves, R. P.; Dos Anjos, J. V. *Molecules* 2012, 17, 5882.
- [12] Senger, M. R.; Gomes, L. C. A.; Ferreira, S. B.; Kaiser, C. R.; Ferreira, V. F.; Silva, F. P. Jr. *Chem Bio Chem* 2012, 13, 1584.
- [13] Shanmugavelan, P.; Nagarajan, S.; Sathishkumar, M.; Ponnuswamy, A.; Yogeewari, P.; Sriram, D. *Bioorg Med Chem Lett* 2011, 21, 7273.
- [14] Kolb, H. C.; Sharpless, K. B. *Drug Discov Today* 2003, 8, 1128.
- [15] (a) Pandeya, S. N.; Smitha, S.; Jyoti, M.; Sridhar, S. K. *Acta Pharm* 2005, 55, 27; (b) Abadi, A. H.; Abou-Seri, S. M.; Abdel-Rahman, D. E.; Klein, C.; Lozach, O.; Meijer, L. *Eur J Med Chem* 2006, 41, 296.
- [16] Singh, P.; Sharma, P.; Anand, A.; Bedi, P. M. S.; Kaur, T.; Saxena, A. K.; Kumar, V. *Eur J Med Chem* 2012, 55, 455.
- [17] Raj, R.; Singh, P.; Singh, P.; Gut, J.; Rosenthal, P. J.; Kumar, V. *Eur J Med Chem* 2013, 62, 590.
- [18] Raj, R.; Singh, P.; Haberkern, N. T.; Faucher, R. M.; Patel, N.; Land, K. M.; Kumar, V. *Eur J Med Chem* 2013, 63, 897.
- [19] Chu, W.; Rothfuss, J.; Zhou, D.; Mach, R. H. *Bioorg Med Chem Lett* 2011, 21, 2192.
- [20] Global tuberculosis control: WHO report 2014.
- [21] Wiid, I.; Seaman, T.; Hoal, E. G.; Benade, A. J. S.; Helden, P. D. V. *IUBMB Life* 2004, 56, 101.
- [22] (a) Shaikh, M. H.; Subhedar, D. D.; Nawale, L.; Sarkar, D.; Khan, F. A. K.; Sangshetti, J. N.; Shingate, B. B. *Med Chem Commun* 2015, 6, 1104; (b) Shingate, B. B.; Hazra, B. G.; Salunke, D. B.; Pore, V. S.; Shirazi, F.; Deshpande, M. V. *Eur J Med Chem* 2011, 46, 3681; (c) Kategaonkar, A. H.; Shinde, P. V.; Kategaonkar, A. H.; Pasale, S. K.; Shingate, B. B.; Shingare, M. S. *Eur J Med Chem* 2010, 45, 3142.
- [23] Alvarez, S. G.; Alvarez, M. T. *Synthesis* 1997, 4, 413.
- [24] Nithinchandra Kalluraya, B.; Shetty, S.; Babu, M. *J Chem Pharm Res* 2013, 5, 307.
- [25] Greenwood, D.; Slack, R. C. B.; Peutherer, J. F. *Medical Microbiology*, 14th ed.; ELBS: London, 1992.
- [26] Singh, U.; Akhtar, S.; Mishra, A.; Sarkar, D. *J Microbiol Methods* 2011, 84, 202.
- [27] Burits, M.; Bucar, F. *Phytother Res* 2000, 14, 323.
- [28] Alley, M. C.; Scudiere, D. A.; Monks, A.; Hursey, M. L.; Czerwinski, M. J.; Fine, D. L.; Abbott, B. J.; Mayo, J. G.; Shoemaker, R. H.; Boyd, M. R. *Cancer Res* 1988, 48, 589.
- [29] Ertl, P.; Rohde, B.; Selzer, P. *J Med Chem* 2000, 43, 3714.
- [30] Strushkevich, N.; Usanov, S. A.; Park, H. W. *J Mol Biol* 2010, 397, 1067.
- [31] Hoofit, R. W.; Vriend, G.; Sander, C.; Abola, E. E. *Nature* 1996, 381, 272.